The nature and origin of the Brucejack high-grade epithermal gold deposit, British Columbia, Canada

D.F. McLeish[1], A.E. Williams-Jones[1], W.S. Board[2], and J.R. Clark[1]

[1]Department of Earth and Planetary Sciences, McGill University, Montréal, Québec, Canada, H3A 0E8
[2]Pretium Resources Inc., Vancouver, British Columbia, Canada, V7X 1L4

I. Location and Tectonostratigraphic Setting

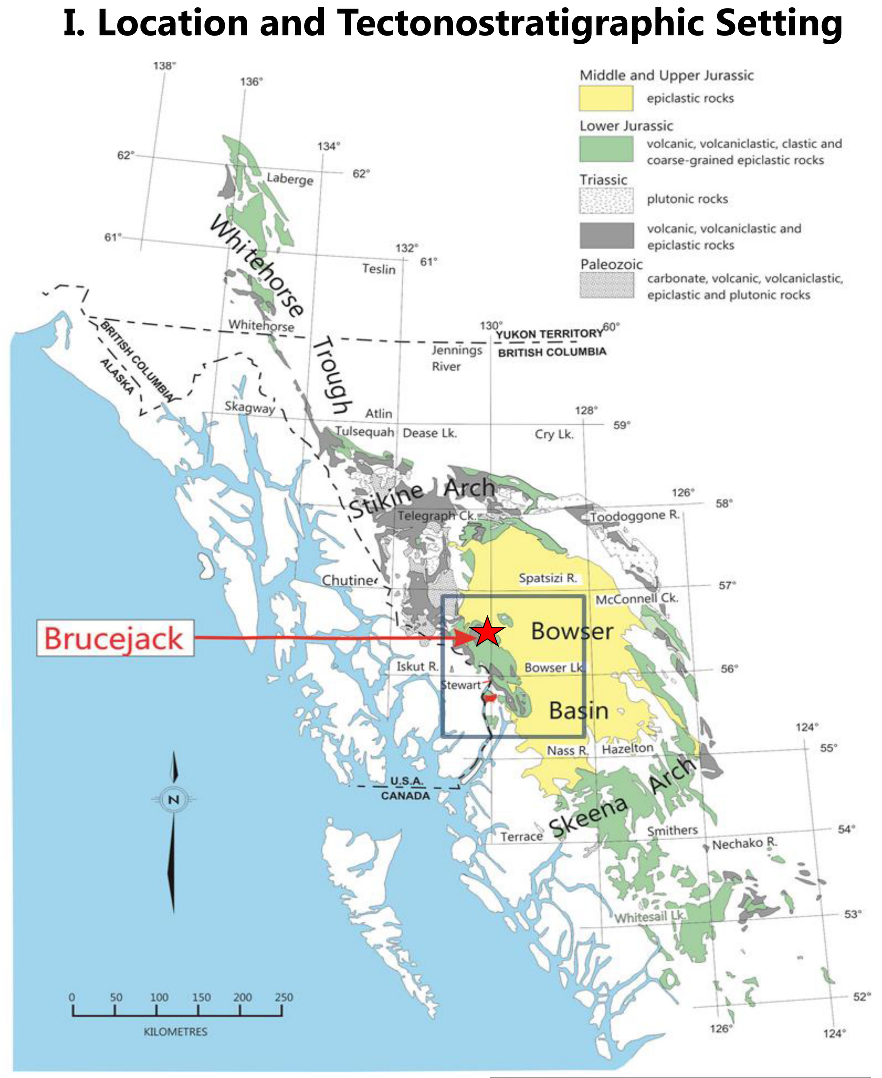

Above: Paleozoic-Jurassic tectonostratigraphic subdivisions of the Stikine terrane in northwestern British Columbia. The Brucejack deposit is hosted within volcano-sedimentary rocks of the Lower Jurassic Hazelton Group on the western margin of the Middle Jurassic Bowser Basin.

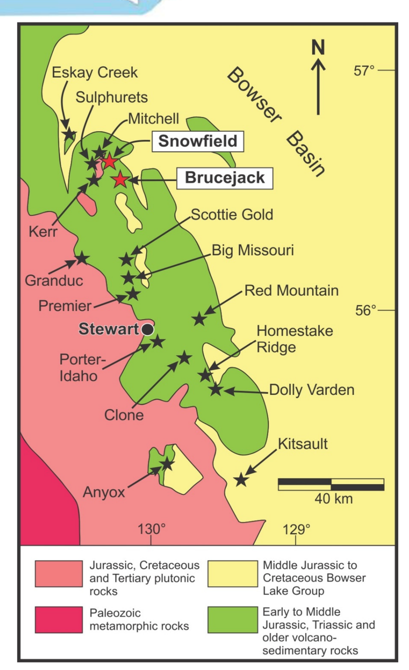

Right: Map showing major deposits of the Stewart-Eskay Creek mining district. Brucejack is located at the northern end of the McTagg anticlinorium, a mid-Cretaceous, regional scale NW-SE trending structural culmination of predominantly Early to Middle Jurassic and Triassic volcano-sedimentary rocks in the western Skeena Fold Belt. Map area is approximately the size of the box in above figure.

II. Deposit Overview

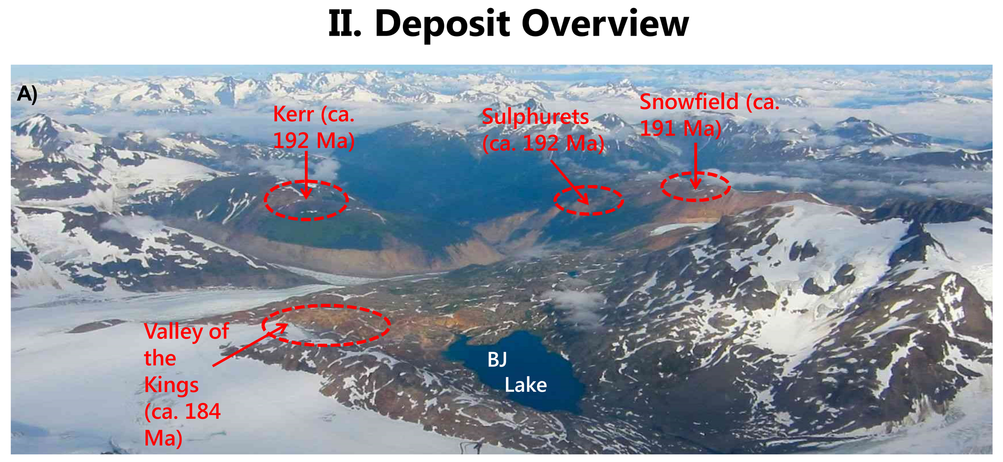

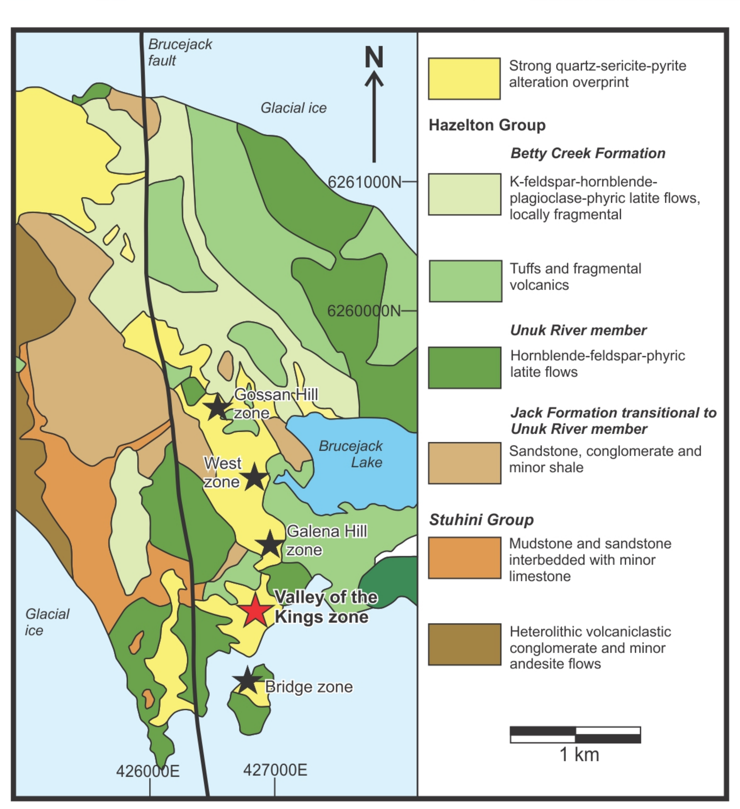

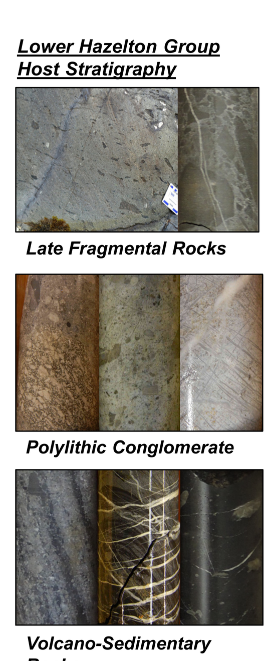

Above: (A) Aerial photo of the Brucejack area showing the location of the Valley of the Kings (VOK) zone relative to neighbouring world-class Cu-Au+/-Mo porphyry deposits. Also visible are the well-developed phyllic alteration-related gossans which are characteristic of deposits in the Sulphurets camp.

(B) The geology of the Brucejack area showing five main zones of mineralisation, which are hosted within a moderately to strongly sericite-quartz-pyrite altered sequence of hornblende and/or feldspar-phyric volcanic flows, lapilli tuffs, locally derived pyroclastic and volcanic conglomerate, sandstone, siltstone, and mudstone of the lowermost Hazelton Group. The zones are proximal to the regional-scale unconformity between the Stuhini and Hazelton groups (after Tombe, 2015).

III. Motivation & Objectives

- **A major challenge in understanding the genesis of epithermal gold deposits is that existing genetic models do not satisfactorily explain the mechanisms responsible for ultra-high gold grades at temperatures characteristic of the epithermal realm (150–300°C).**
- **Dissolution in an hydrothermal liquid is the widely proposed mechanism for mobilizing gold within the crust (e.g., Krupp & Seward, 1987; Sillitoe & Hedenquist, 2003; Williams-Jones et al., 2009).**
- **However, experiments have shown that the solubility of gold is too low in hydrothermal liquids at temperatures < ~ 400°C to account for the extreme grades observed in some epithermal deposits (e.g. Gammons and Williams-Jones, 1995).**
- **Alternative explanations for the extreme grades observed in deposits such as Brucejack (where diamond drilling has returned grades up to 41,582 g/t Au over 0.5 m intervals) involve scenarios wherein:**
  - **(1) the temperatures commonly assumed for gold transport greatly underestimate the true temperature because they are based on estimates of the conditions of deposition;**
  - **(2) high fluid fluxes and steep physicochemical gradients can be maintained in single fractures for exceptionally long periods of time (unlikely);**
  - **(3) the capacity of a fluid to transport gold is not controlled by simple solubility, either in a vapour or a liquid, but is also controlled by other processes. For example, the development of boiling-mediated nanoparticle suspensions (colloids) could greatly increase the capacity of the fluid to carry gold.**
- **Our study is currently using EMP, LA-ICP-MS, and TEM methods to test plausible models for ore formation at Brucejack and gain insight into the physicochemical evolution of the deposit. Ultimately, we aim address the fundamental question of whether the large, high-grade Brucejack resource can be formed using simple solubility considerations.**

IV. Background: Hydrothermal Transport & Deposition of Gold from Solution

- Transport: Gold bonds preferentially with soft ligands like HS^- at temperatures characteristic of the epithermal realm (150–300°C). At higher temperatures, such as those characteristics of the porphyry environment, $AuCl^-$ species predominate.
- Deposition: deposition (precipitation) of gold from solution is controlled by the following reactions in the epithermal realm:

$$Au_S + HS^- + H^+ + 1/4\ O_2 \rightleftharpoons Au(HS)^\circ + 1/2\ H_2O \qquad (1)$$

$$Au_S + 2HS^- + H^+ + 1/4\ O_2 \rightleftharpoons Au(HS)_2^- + 1/2\ H_2O \qquad (2)$$

- Decreasing aHS^- and fO_2 and/or increasing pH will promote deposition of gold from solution by driving these reactions to the left, as per Le Châtelier's principle.

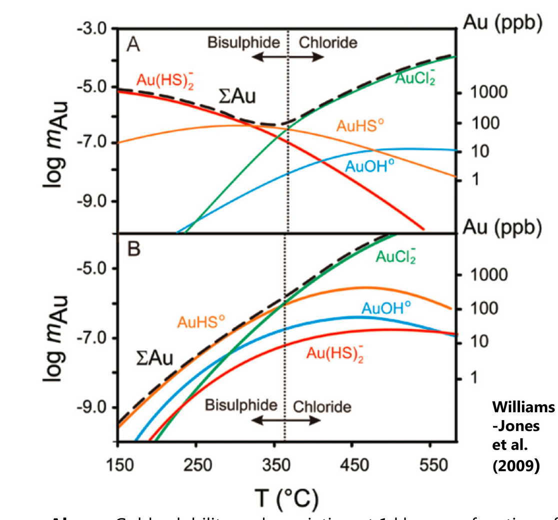

Above: Gold solubility and speciation at 1 kbar as a function of temperature for an aqueous solution containing 1.5 m NaCl and 0.5 m KCl. (A) ΣS (total S) = 0.01 m and fO_2 is buffered by the assemblage hematite–magnetite. (B) ΣS and fO_2 are buffered by the assemblage pyrite–pyrrhotite–magnetite; the maximum value of ΣS is 0.1 m.

- Such changes in physicochemical conditions in epithermal deposits are commonly achieved by:
  - Boiling: fractionation of H_2S to vapour decreases aHS^-
  - Magmatic-meteoric fluid mixing: the pH of a magmatic-hydrothermal system is increased by infiltration and mixing of higher pH meteoric water with magmatic fluid; this also leads to a decrease in temperature.
  - Mafic wallrock sulphidation: Fe-silicate and Fe-oxide minerals in the wallrock of a deposit are altered to pyrite by a H_2S bearing fluid, thereby decreasing aHS^- of the fluid as per the following reaction:

$$Fe^{2+} + 2\ H_2S + ½\ O_2 = FeS_2 + 2\ H^+ + H_2O$$

V. Early Invisible Gold Mineralisation in Arsenian Pyrite

Below: Early, invisible gold mineralisation at Brucejack occurs in arsenic-rich laminae within oscillatory zoned pyrite. This pyrite is found both within strongly sulphidised wallrocks as well as within the main mineralisation-stage, quartz-carbonate-electrum veins. Electrum mineralisation cross-cuts the gold-bearing arsenian pyrite laminae within the quartz-carbonate-electrum veins (Box VIII). Pre-electrum deformation of the arsenian pyrite is locally observed (lowermost left). All images are backscattered-electron (BSE) images; images on the right show EMP-WDS analysis spots with corresponding results for As, Au, Cu, Fe, and S (detection limit for Au is 0.01 wt%).

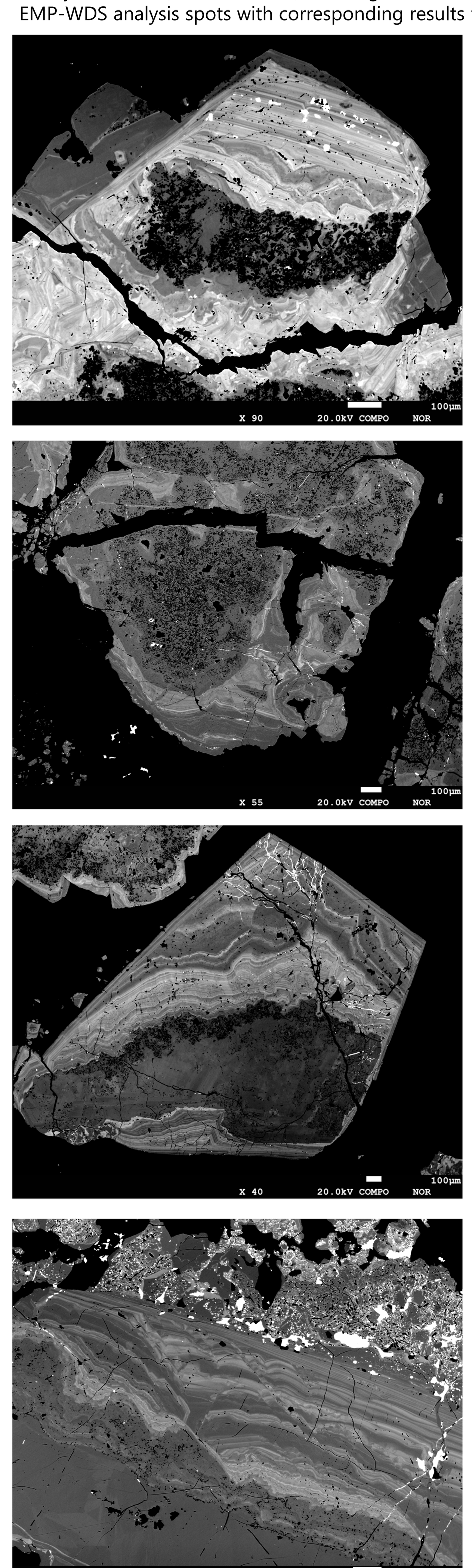

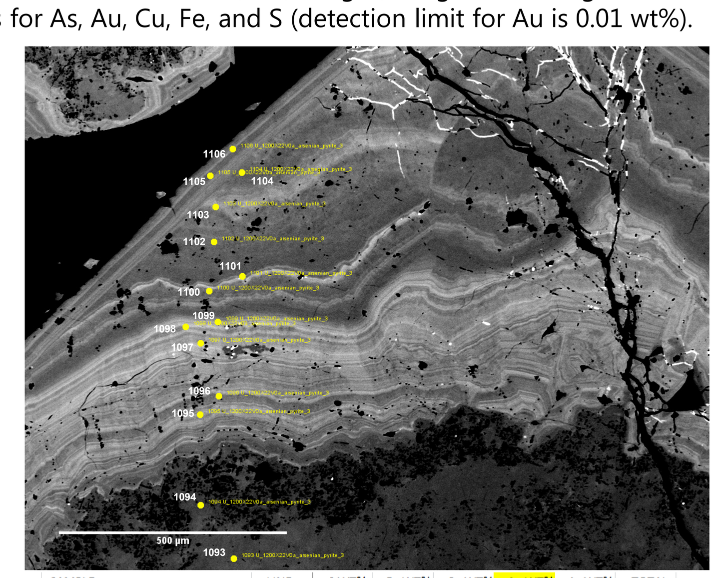

SAMPLE	LINE	S WT%	Fe WT%	Cu WT%	Au WT%	As WT%	TOTAL
U_1200X22V0a_arsenian_pyrite_3	1106	49.96	44.07	3.81	0.003	2.00	99.83
U_1200X22V0a_arsenian_pyrite_3	1105	52.50	45.96	-	0.005	0.94	99.41
U_1200X22V0a_arsenian_pyrite_3	1104	52.63	46.10	0.00	0.005	0.90	99.64
U_1200X22V0a_arsenian_pyrite_3	1103	52.45	46.08	0.01	-	1.21	99.75
U_1200X22V0a_arsenian_pyrite_3	1102	52.34	46.15	0.00	-	1.34	99.84
U_1200X22V0a_arsenian_pyrite_3	1101	50.76	45.48	0.00	0.014	3.28	99.53
U_1200X22V0a_arsenian_pyrite_3	1100	52.76	46.09	-	-	0.82	99.67
U_1200X22V0a_arsenian_pyrite_3	1099	50.33	45.29	0.01	0.005	3.88	99.51
U_1200X22V0a_arsenian_pyrite_3	1098	51.78	45.96	-	-	2.04	99.78
U_1200X22V0a_arsenian_pyrite_3	1097	50.27	45.38	0.01	0.012	3.93	99.59
U_1200X22V0a_arsenian_pyrite_3	1096	52.34	46.05	-	0.020	1.37	99.77
U_1200X22V0a_arsenian_pyrite_3	1095	50.91	45.61	0.01	0.021	3.19	99.74
U_1200X22V0a_arsenian_pyrite_3	1094	53.13	46.34	-	-	0.47	99.95

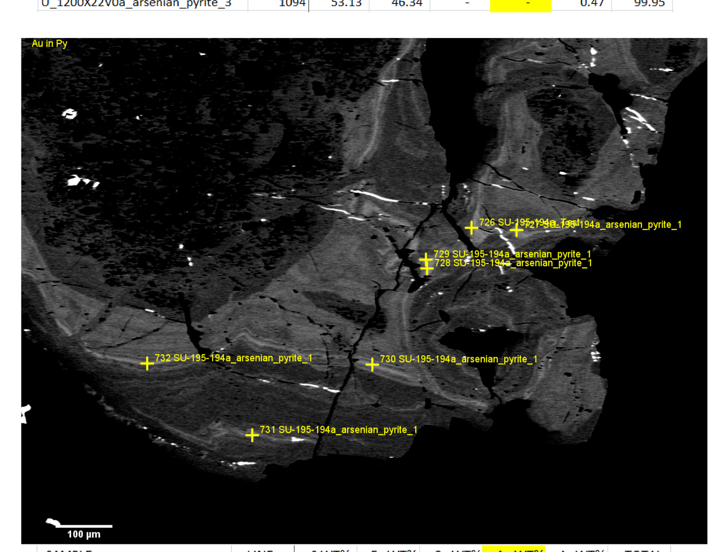

SAMPLE	LINE	S WT%	Fe WT%	Cu WT%	Au WT%	As WT%	TOTAL
SU-195-194a_arsenian_pyrite_1	726	51.03	46.53	0.02	0.021	3.44	101.03
SU-195-194a_arsenian_pyrite_1	727	51.24	46.70	0.01	0.033	3.41	101.39
SU-195-194a_arsenian_pyrite_1	728	51.41	46.61	0.02	0.029	3.36	101.43
SU-195-194a_arsenian_pyrite_1	729	51.37	46.65	0.02	0.026	3.39	101.45
SU-195-194a_arsenian_pyrite_1	730	51.53	46.62	0.02	0.042	3.10	101.30
SU-195-194a_arsenian_pyrite_1	731	52.02	46.52	0.01	0.015	2.54	101.11
SU-195-194a_arsenian_pyrite_1	732	51.81	46.61	0.02	0.028	2.89	101.35

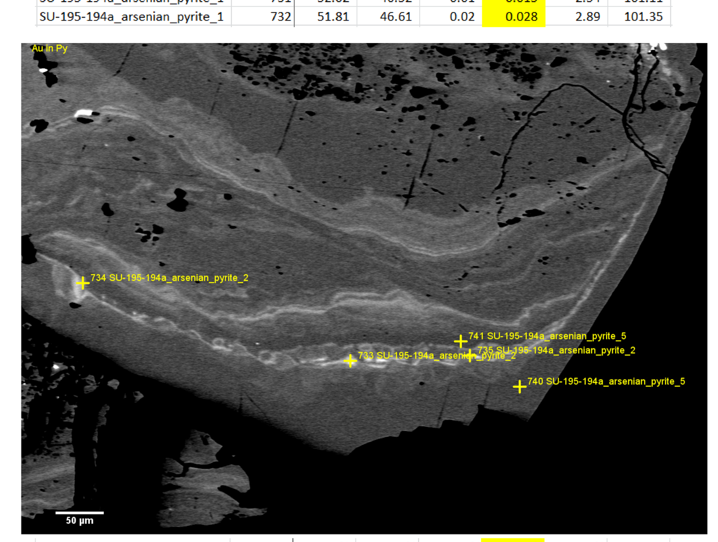

SAMPLE	LINE	S WT%	Fe WT%	Cu WT%	Au WT%	As WT%	TOTAL
SU-195-194a_arsenian_pyrite_2	733	50.81	45.82	0.01	0.024	3.97	100.63
SU-195-194a_arsenian_pyrite_2	734	50.88	46.16	0.01	0.015	4.43	101.50
SU-195-194a_arsenian_pyrite_2	735	52.42	45.70	0.11	0.192	0.92	99.34
SU-195-194a_arsenian_pyrite_5	740	54.33	48.58	-	-	0.01	102.92
SU-195-194a_arsenian_pyrite_5	741	54.25	47.45	-	0.000	-	101.69

VI. Evidence for possible porphyry origin of early invisible gold

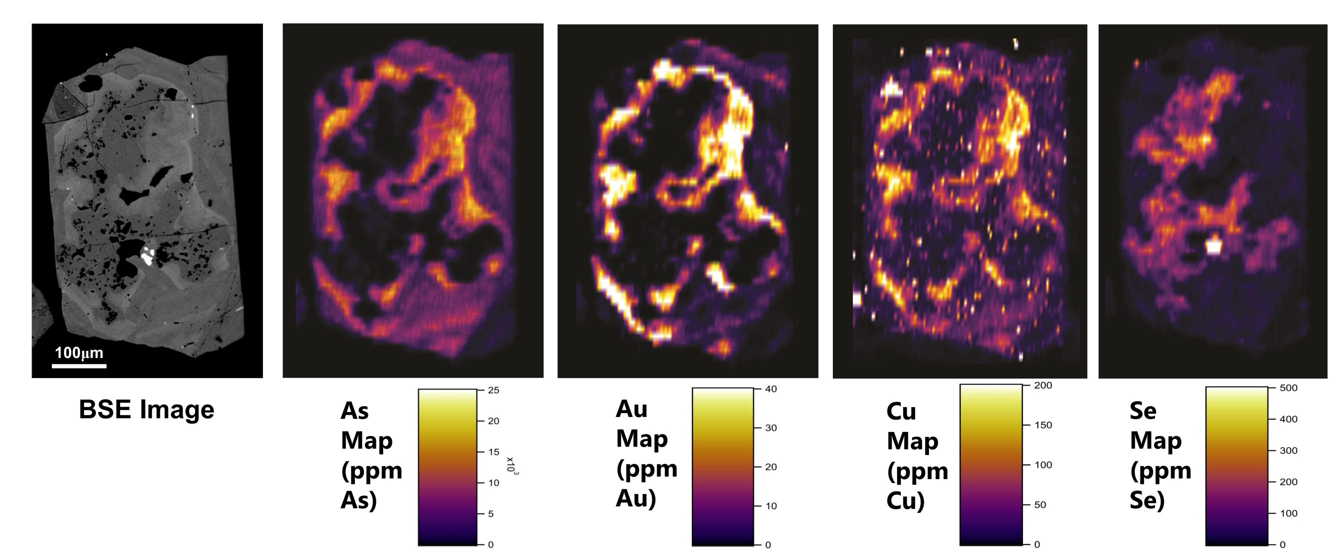

1st Zone (core)	2nd zone (High As - irregular/anhedral zonation)	3rd zone (Outer)
Se	As	Ni
Sb	Au	Co
Pb	Cu	Th
Bi	(+/-) Mo	
(+/-) Ag	(+/-) Hg	
(+/-) Ge		

Above: Laser-ablation inductively coupled plasma–mass spectrometry (LA-ICP-MS) mapping of Brucejack pyrite shows the intermediate zone of oscillatory zoned arsenian pyrite to have a geochemical signature consistent with a porphyry source (Cu, As, +/- Mo). This observation, coupled with the observation of electrum cross-cutting auriferous, oscillatory-zoned arsenian pyrite (Box VIII), suggests that at least the first two generations of pyrite growth at Brucejack predated the quartz-carbonate-electrum epithermal veining events and may be related to a phyllic alteration halo surrounding the older, neighbouring porphyry deposits of the Sulphurets camp (Kerr, Sulphurets, Mitchell, and Snowfield deposits).

VII. Nanoparticulate electrum

Below: Transmission Electron Microscopic (TEM) imaging of silica- and carbonate-contaminated electrum (**A & B**, EMP element map and BSE image, respectively) from Vn1 veins at Brucejack has revealed the presence of ~ < 1 to 10 nm wide spheres of electrum within these veins (**C & D**, low-magnification and high-resolution TEM images, respectively). The lattice spacing within these nanocrystals varies between 2.2 and 2.4 Å (**E**, HRTEM image of upper-left particle in D), which is consistent with the lattice spacing for electrum. Larger particles (**F**, HRTEM image), display multiple lattice orientations suggesting they may have formed through the flocculation of numerous, smaller nanocrystals.

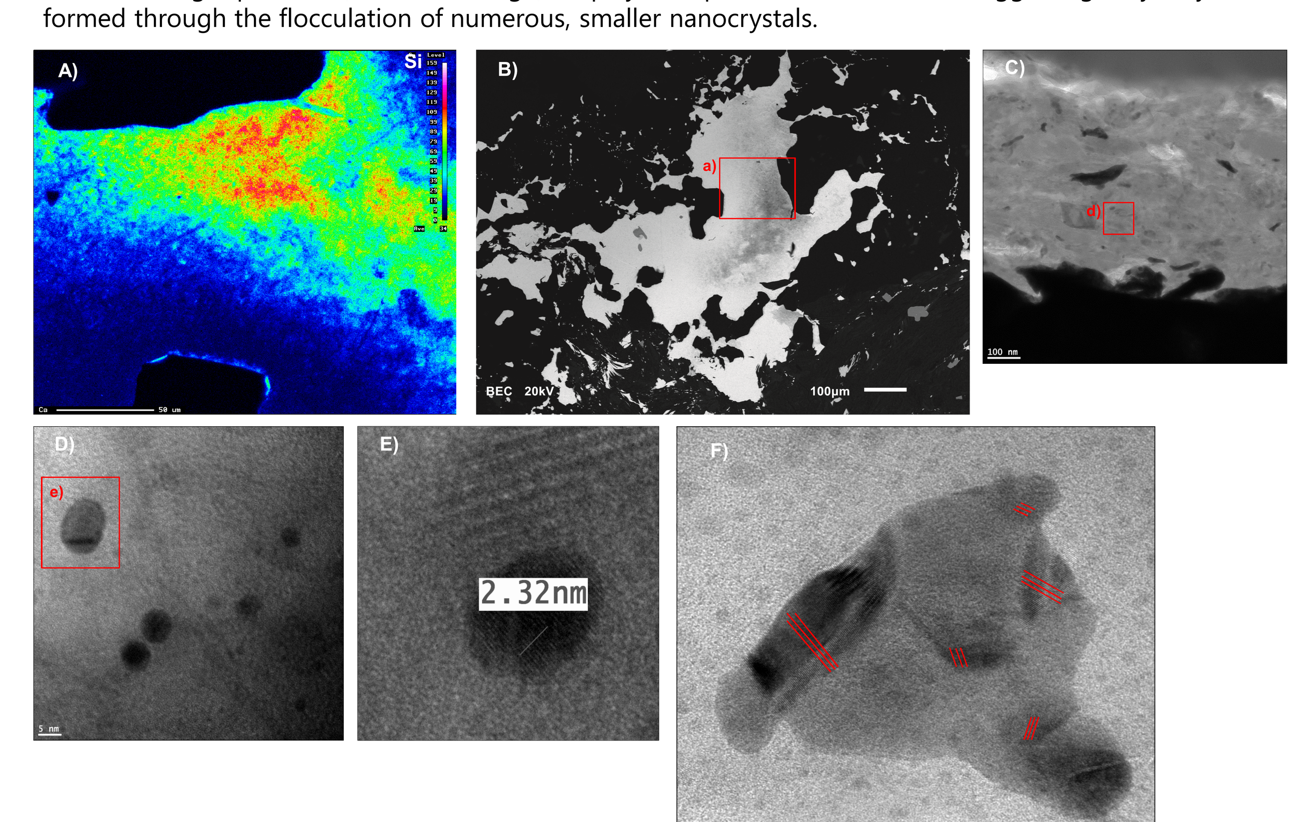

VIII. Late Free Gold (electrum) Mineralisation

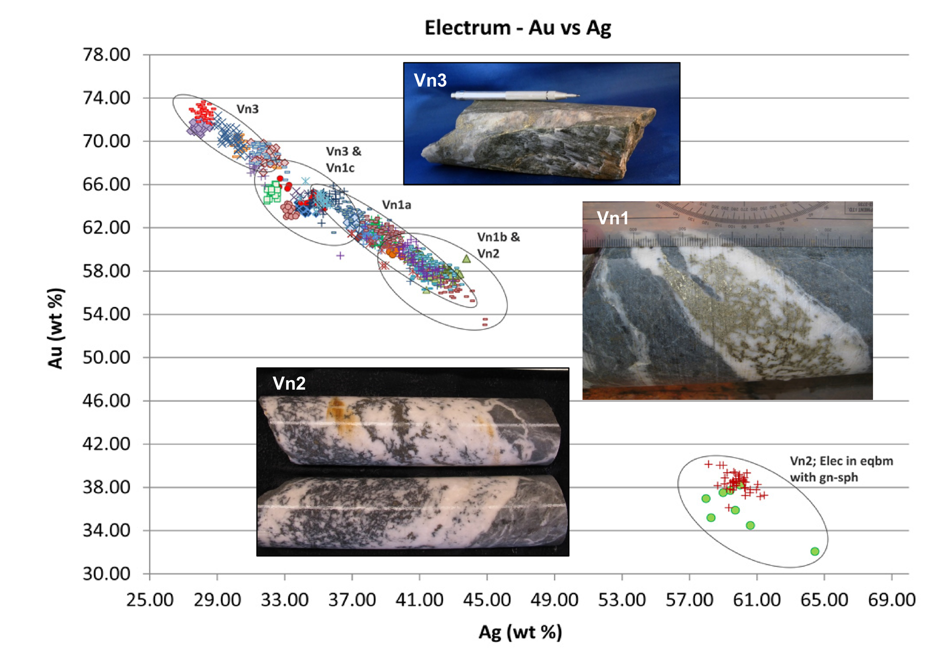

Above: Electrum (Au, Ag) at Brucejack is hosted in five vein stages and sub-stages: 1) electrum-bearing quartz–carbonate±sericite sheeted, stockwork and brecciated veins (Vn1a, Vn1b and Vn1c, respectively); 2) zinc–lead±copper sulphide veins containing abundant silver sulphosalts and electrum (Vn2); and 3) carbonate±quartz veins containing orange-coloured, manganese-bearing calcite, and electrum (Vn3). A binary Au/Ag plot of electron microprobe WDS analyses of Brucejack electrum shows that there is significant variability of the Au/Ag ratio of electrum among vein stages.

Below: Oscillatory zoned pyrite from Vn1 veins is cross-cut and possibly locally replaced by veinlets of electrum (bright mineral; BSE images).

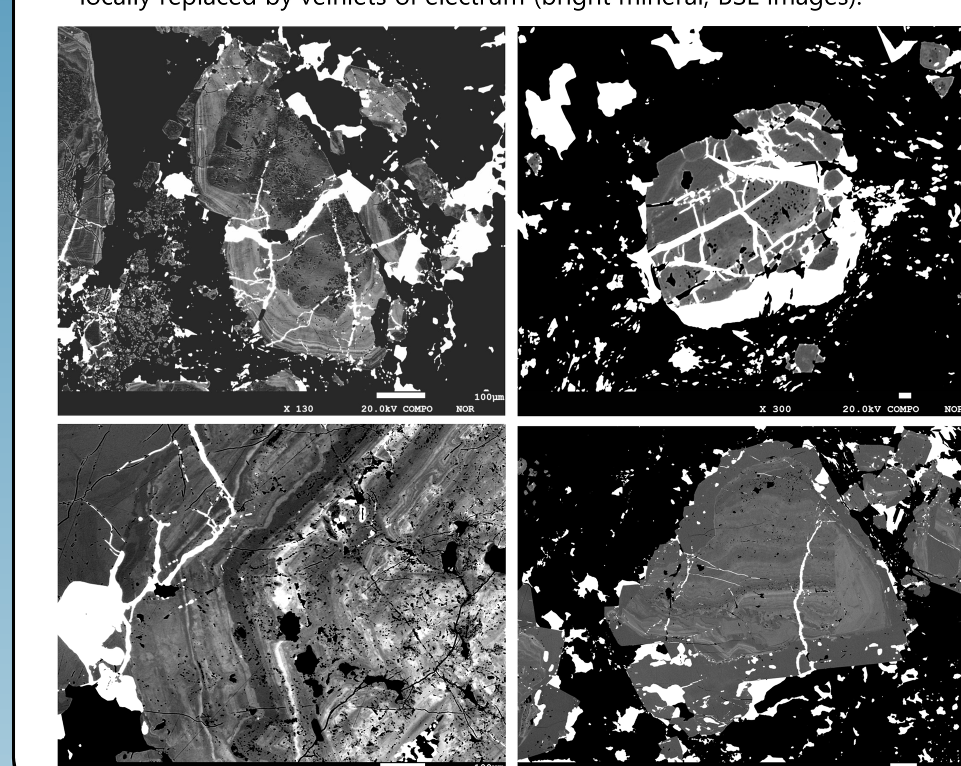

IX. Preliminary Conclusions & Future Work

- **The formation of five syn-mineral vein stages and sub-stages appears to have resulted from multiple pulses of fluid that circulated through the deposit under dynamic physicochemical conditions.**
- **Analyses of pre-electrum pyrite using EMP-WDS and LA-ICP-MS methods show that arsenic-rich growth zones contain up to 1920 ppm gold, indicating that auriferous pyrite mineralisation, likely related to a phyllic alteration of the volcano-sedimentary country rocks surrounding older neighboring porphyry deposits, was partially responsible for the 8.7 million ounce gold reserve at Brucejack.**
- **Preliminary transmission electron microscopic (TEM) imaging has revealed the presence of spherical nanocrystals of electrum within these veins, suggesting that nanoparticle suspensions (colloids) produced by boiling may have played a role in greatly increasing the capacity of the ore-forming fluid to carry gold by allowing for its physical transport.**
- **Future petrographic, mineral-chemistry, and fluid-inclusion studies will further test these interpretations and search for other insights into the physicochemical evolution of the Brucejack deposit. We plan to use data from these investigations to reconstruct the physicochemical conditions that controlled mineralisation through thermodynamic analysis, and quantitatively test plausible models of ore formation.**

X. Acknowledgements & References

Overview maps in Section 1 and aerial photo in Section 2 are adapted from a Pretium Resources Inc. technical presentation:

Board, W.S. (2015): Geology update on the Brucejack High Grade Au-Ag deposit Northwestern British Columbia, Canada. Pretium Resources Inc. internal technical presentation. Vancouver, Canada.

Other references cited:

Gammons, C.H. and Williams-Jones, A.E (1995): The solubility of Au-Ag alloy + AgCl in HCl/NaCl solutions at 300°C: New data on the stability of Au (1) chloride complexes in hydrothermal fluids; Geochimica et Cosmochimica Acta, v. 59, p. 3453-3468.

Krupp, R.E., and Seward, T.M. (1987): The Rotokawa geothermal system, New Zealand: an active epithermal ore-depositing environment; Economic Geology, v. 82, p. 1109–1129.

Sillitoe, R.H. and Hedenquist, J. W. (2003): Linkages between volcanotectonic settings, ore-fluid compositions, and epithermal precious metal deposits; in Volcanic, Geothermal, and Ore-Forming Fluids: Rulers and Witnesses of Processes within the Earth, S.F. Simmons and I. Graham (ed.), SEG Special Publication 10, p. 315–345.

Tombe, S.P. (2015): Age and origin of the Brucejack epithermal Au-Ag deposit, northwestern British Columbia. M.Sc. thesis, University of Alberta.

Williams-Jones A.E., Bowell R.J., Migdisov, A.A. (2009): Gold in Solution. Elements 5(5): 281-287.

Project funding provided by Pretium Resources Inc. and:

Geoscience BC

NSERC CRSNG